arXiv:hep-ex/0307026v2 4 Nov 2003

Rates, Polarizations, and Asymmetries in Charmless Vector-Vector B Meson Decays

B. Aubert,[1] R. Barate,[1] D. Boutigny,[1] J.-M. Gaillard,[1] A. Hicheur,[1] Y. Karyotakis,[1] J. P. Lees,[1] P. Robbe,[1]
V. Tisserand,[1] A. Zghiche,[1] A. Palano,[2] A. Pompili,[2] J. C. Chen,[3] N. D. Qi,[3] G. Rong,[3] P. Wang,[3] Y. S. Zhu,[3]
G. Eigen,[4] I. Ofte,[4] B. Stugu,[4] G. S. Abrams,[5] A. W. Borgland,[5] A. B. Breon,[5] D. N. Brown,[5] J. Button-Shafer,[5]
R. N. Cahn,[5] E. Charles,[5] C. T. Day,[5] M. S. Gill,[5] A. V. Gritsan,[5] Y. Groysman,[5] R. G. Jacobsen,[5] R. W. Kadel,[5]
J. Kadyk,[5] L. T. Kerth,[5] Yu. G. Kolomensky,[5] J. F. Kral,[5] G. Kukartsev,[5] C. LeClerc,[5] M. E. Levi,[5] G. Lynch,[5]
L. M. Mir,[5] P. J. Oddone,[5] T. J. Orimoto,[5] M. Pripstein,[5] N. A. Roe,[5] A. Romosan,[5] M. T. Ronan,[5] V. G. Shelkov,[5]
A. V. Telnov,[5] W. A. Wenzel,[5] K. Ford,[6] T. J. Harrison,[6] C. M. Hawkes,[6] D. J. Knowles,[6] S. E. Morgan,[6]
R. C. Penny,[6] A. T. Watson,[6] N. K. Watson,[6] T. Deppermann,[7] K. Goetzen,[7] H. Koch,[7] B. Lewandowski,[7]
M. Pelizaeus,[7] K. Peters,[7] H. Schmuecker,[7] M. Steinke,[7] N. R. Barlow,[8] J. T. Boyd,[8] N. Chevalier,[8]
W. N. Cottingham,[8] M. P. Kelly,[8] T. E. Latham,[8] C. Mackay,[8] F. F. Wilson,[8] K. Abe,[9] T. Cuhadar-Donszelmann,[9]
C. Hearty,[9] T. S. Mattison,[9] J. A. McKenna,[9] D. Thiessen,[9] P. Kyberd,[10] A. K. McKemey,[10] V. E. Blinov,[11]
A. D. Bukin,[11] V. B. Golubev,[11] V. N. Ivanchenko,[11] E. A. Kravchenko,[11] A. P. Onuchin,[11] S. I. Serednyakov,[11]
Yu. I. Skovpen,[11] E. P. Solodov,[11] A. N. Yushkov,[11] D. Best,[12] M. Chao,[12] D. Kirkby,[12] A. J. Lankford,[12]
M. Mandelkern,[12] S. McMahon,[12] R. K. Mommsen,[12] W. Roethel,[12] D. P. Stoker,[12] C. Buchanan,[13] D. del
Re,[14] H. K. Hadavand,[14] E. J. Hill,[14] D. B. MacFarlane,[14] H. P. Paar,[14] Sh. Rahatlou,[14] U. Schwanke,[14]
V. Sharma,[14] J. W. Berryhill,[15] C. Campagnari,[15] B. Dahmes,[15] N. Kuznetsova,[15] S. L. Levy,[15] O. Long,[15]
A. Lu,[15] M. A. Mazur,[15] J. D. Richman,[15] W. Verkerke,[15] T. W. Beck,[16] J. Beringer,[16] A. M. Eisner,[16]
C. A. Heusch,[16] W. S. Lockman,[16] T. Schalk,[16] R. E. Schmitz,[16] B. A. Schumm,[16] A. Seiden,[16] M. Turri,[16]
W. Walkowiak,[16] D. C. Williams,[16] M. G. Wilson,[16] J. Albert,[17] E. Chen,[17] G. P. Dubois-Felsmann,[17]
A. Dvoretskii,[17] D. G. Hitlin,[17] I. Narsky,[17] F. C. Porter,[17] A. Ryd,[17] A. Samuel,[17] S. Yang,[17] S. Jayatilleke,[18]
G. Mancinelli,[18] B. T. Meadows,[18] M. D. Sokoloff,[18] T. Abe,[19] T. Barillari,[19] F. Blanc,[19] P. Bloom,[19] S. Chen,[19]
P. J. Clark,[19] W. T. Ford,[19] U. Nauenberg,[19] A. Olivas,[19] P. Rankin,[19] J. Roy,[19] J. G. Smith,[19] W. C. van Hoek,[19]
L. Zhang,[19] J. L. Harton,[20] T. Hu,[20] A. Soffer,[20] W. H. Toki,[20] R. J. Wilson,[20] J. Zhang,[20] D. Altenburg,[21]
T. Brandt,[21] J. Brose,[21] T. Colberg,[21] M. Dickopp,[21] R. S. Dubitzky,[21] A. Hauke,[21] H. M. Lacker,[21] E. Maly,[21]
R. Müller-Pfefferkorn,[21] R. Nogowski,[21] S. Otto,[21] K. R. Schubert,[21] R. Schwierz,[21] B. Spaan,[21] L. Wilden,[21]
D. Bernard,[22] G. R. Bonneaud,[22] F. Brochard,[22] J. Cohen-Tanugi,[22] Ch. Thiebaux,[22] G. Vasileiadis,[22] M. Verderi,[22]
A. Khan,[23] D. Lavin,[23] F. Muheim,[23] S. Playfer,[23] J. E. Swain,[23] J. Tinslay,[23] M. Andreotti,[24] V. Azzolini,[24]
D. Bettoni,[24] C. Bozzi,[24] R. Calabrese,[24] G. Cibinetto,[24] E. Luppi,[24] M. Negrini,[24] L. Piemontese,[24] A. Sarti,[24]
E. Treadwell,[25] F. Anulli,[26, *] R. Baldini-Ferroli,[26] A. Calcaterra,[26] R. de Sangro,[26] D. Falciai,[26] G. Finocchiaro,[26]
P. Patteri,[26] I. M. Peruzzi,[26, *] M. Piccolo,[26] A. Zallo,[26] A. Buzzo,[27] R. Contri,[27] G. Crosetti,[27] M. Lo Vetere,[27]
M. Macri,[27] M. R. Monge,[27] S. Passaggio,[27] F. C. Pastore,[27] C. Patrignani,[27] E. Robutti,[27] A. Santroni,[27]
S. Tosi,[27] S. Bailey,[28] M. Morii,[28] W. Bhimji,[29] D. A. Bowerman,[29] P. D. Dauncey,[29] U. Egede,[29] I. Eschrich,[29]
J. R. Gaillard,[29] G. W. Morton,[29] J. A. Nash,[29] P. Sanders,[29] G. P. Taylor,[29] G. J. Grenier,[30] S.-J. Lee,[30]
U. Mallik,[30] J. Cochran,[31] H. B. Crawley,[31] J. Lamsa,[31] W. T. Meyer,[31] S. Prell,[31] E. I. Rosenberg,[31] J. Yi,[31]
M. Davier,[32] G. Grosdidier,[32] A. Höcker,[32] S. Laplace,[32] F. Le Diberder,[32] V. Lepeltier,[32] A. M. Lutz,[32]
T. C. Petersen,[32] S. Plaszczynski,[32] M. H. Schune,[32] L. Tantot,[32] G. Wormser,[32] V. Brigljević,[33] C. H. Cheng,[33]
D. J. Lange,[33] D. M. Wright,[33] A. J. Bevan,[34] J. P. Coleman,[34] J. R. Fry,[34] E. Gabathuler,[34] R. Gamet,[34]
M. Kay,[34] R. J. Parry,[34] D. J. Payne,[34] R. J. Sloane,[34] C. Touramanis,[34] J. J. Back,[35] P. F. Harrison,[35]
H. W. Shorthouse,[35] P. Strother,[35] P. B. Vidal,[35] C. L. Brown,[36] G. Cowan,[36] R. L. Flack,[36] H. U. Flaecher,[36]
S. George,[36] M. G. Green,[36] A. Kurup,[36] C. E. Marker,[36] T. R. McMahon,[36] S. Ricciardi,[36] F. Salvatore,[36]
G. Vaitsas,[36] M. A. Winter,[36] D. Brown,[37] C. L. Davis,[37] J. Allison,[38] R. J. Barlow,[38] A. C. Forti,[38] P. A. Hart,[38]
F. Jackson,[38] G. D. Lafferty,[38] A. J. Lyon,[38] J. H. Weatherall,[38] J. C. Williams,[38] A. Farbin,[39] A. Jawahery,[39]
D. Kovalskyi,[39] C. K. Lae,[39] V. Lillard,[39] D. A. Roberts,[39] G. Blaylock,[40] C. Dallapiccola,[40] K. T. Flood,[40]
S. S. Hertzbach,[40] R. Kofler,[40] V. B. Koptchev,[40] T. B. Moore,[40] S. Saremi,[40] H. Staengle,[40] S. Willocq,[40]
R. Cowan,[41] G. Sciolla,[41] F. Taylor,[41] R. K. Yamamoto,[41] D. J. J. Mangeol,[42] M. Milek,[42] P. M. Patel,[42]
A. Lazzaro,[43] F. Palombo,[43] J. M. Bauer,[44] L. Cremaldi,[44] V. Eschenburg,[44] R. Godang,[44] R. Kroeger,[44]

J. Reidy,[44] D. A. Sanders,[44] D. J. Summers,[44] H. W. Zhao,[44] C. Hast,[45] P. Taras,[45] H. Nicholson,[46] C. Cartaro,[47] N. Cavallo,[47, †] G. De Nardo,[47] F. Fabozzi,[47, †] C. Gatto,[47] L. Lista,[47] P. Paolucci,[47] D. Piccolo,[47] C. Sciacca,[47] M. A. Baak,[48] G. Raven,[48] J. M. LoSecco,[49] T. A. Gabriel,[50] B. Brau,[51] T. Pulliam,[51] Q. K. Wong,[51] J. Brau,[52] R. Frey,[52] C. T. Potter,[52] N. B. Sinev,[52] D. Strom,[52] E. Torrence,[52] F. Colecchia,[53] A. Dorigo,[53] F. Galeazzi,[53] M. Margoni,[53] M. Morandin,[53] M. Posocco,[53] M. Rotondo,[53] F. Simonetto,[53] R. Stroili,[53] G. Tiozzo,[53] C. Voci,[53] M. Benayoun,[54] H. Briand,[54] J. Chauveau,[54] P. David,[54] Ch. de la Vaissière,[54] L. Del Buono,[54] O. Hamon,[54] M. J. J. John,[54] Ph. Leruste,[54] J. Ocariz,[54] M. Pivk,[54] L. Roos,[54] J. Stark,[54] S. T'Jampens,[54] G. Therin,[54] P. F. Manfredi,[55] V. Re,[55] L. Gladney,[56] Q. H. Guo,[56] J. Panetta,[56] C. Angelini,[57] G. Batignani,[57] S. Bettarini,[57] M. Bondioli,[57] F. Bucci,[57] G. Calderini,[57] M. Carpinelli,[57] F. Forti,[57] M. A. Giorgi,[57] A. Lusiani,[57] G. Marchiori,[57] F. Martinez-Vidal,[57, ‡] M. Morganti,[57] N. Neri,[57] E. Paoloni,[57] M. Rama,[57] G. Rizzo,[57] F. Sandrelli,[57] J. Walsh,[57] M. Haire,[58] D. Judd,[58] K. Paick,[58] D. E. Wagoner,[58] N. Danielson,[59] P. Elmer,[59] C. Lu,[59] V. Miftakov,[59] J. Olsen,[59] A. J. S. Smith,[59] H. A. Tanaka,[59] E. W. Varnes,[59] F. Bellini,[60] G. Cavoto,[59, 60] R. Faccini,[14, 60] F. Ferrarotto,[60] F. Ferroni,[60] M. Gaspero,[60] M. A. Mazzoni,[60] S. Morganti,[60] M. Pierini,[60] G. Piredda,[60] F. Safai Tehrani,[60] C. Voena,[60] S. Christ,[61] G. Wagner,[61] R. Waldi,[61] T. Adye,[62] N. De Groot,[62] B. Franek,[62] N. I. Geddes,[62] G. P. Gopal,[62] E. O. Olaiya,[62] S. M. Xella,[62] R. Aleksan,[63] S. Emery,[63] A. Gaidot,[63] S. F. Ganzhur,[63] P.-F. Giraud,[63] G. Hamel de Monchenault,[63] W. Kozanecki,[63] M. Langer,[63] G. W. London,[63] B. Mayer,[63] G. Schott,[63] G. Vasseur,[63] Ch. Yeche,[63] M. Zito,[63] M. V. Purohit,[64] A. W. Weidemann,[64] F. X. Yumiceva,[64] D. Aston,[65] R. Bartoldus,[65] N. Berger,[65] A. M. Boyarski,[65] O. L. Buchmueller,[65] M. R. Convery,[65] D. P. Coupal,[65] D. Dong,[65] J. Dorfan,[65] D. Dujmic,[65] W. Dunwoodie,[65] R. C. Field,[65] T. Glanzman,[65] S. J. Gowdy,[65] E. Grauges-Pous,[65] T. Hadig,[65] V. Halyo,[65] T. Hryn'ova,[65] W. R. Innes,[65] C. P. Jessop,[65] M. H. Kelsey,[65] P. Kim,[65] M. L. Kocian,[65] U. Langenegger,[65] D. W. G. S. Leith,[65] S. Luitz,[65] V. Luth,[65] H. L. Lynch,[65] H. Marsiske,[65] S. Menke,[65] R. Messner,[65] D. R. Muller,[65] C. P. O'Grady,[65] V. E. Ozcan,[65] A. Perazzo,[65] M. Perl,[65] S. Petrak,[65] B. N. Ratcliff,[65] S. H. Robertson,[65] A. Roodman,[65] A. A. Salnikov,[65] R. H. Schindler,[65] J. Schwiening,[65] G. Simi,[65] A. Snyder,[65] A. Soha,[65] J. Stelzer,[65] D. Su,[65] M. K. Sullivan,[65] J. Va'vra,[65] S. R. Wagner,[65] M. Weaver,[65] A. J. R. Weinstein,[65] W. J. Wisniewski,[65] D. H. Wright,[65] C. C. Young,[65] P. R. Burchat,[66] A. J. Edwards,[66] T. I. Meyer,[66] C. Roat,[66] S. Ahmed,[67] M. S. Alam,[67] J. A. Ernst,[67] M. Saleem,[67] F. R. Wappler,[67] W. Bugg,[68] M. Krishnamurthy,[68] S. M. Spanier,[68] R. Eckmann,[69] H. Kim,[69] J. L. Ritchie,[69] R. F. Schwitters,[69] J. M. Izen,[70] I. Kitayama,[70] X. C. Lou,[70] S. Ye,[70] F. Bianchi,[71] M. Bona,[71] F. Gallo,[71] D. Gamba,[71] C. Borean,[72] L. Bosisio,[72] G. Della Ricca,[72] S. Dittongo,[72] S. Grancagnolo,[72] L. Lanceri,[72] P. Poropat,[72, §] L. Vitale,[72] G. Vuagnin,[72] R. S. Panvini,[73] Sw. Banerjee,[74] C. M. Brown,[74] D. Fortin,[74] P. D. Jackson,[74] R. Kowalewski,[74] J. M. Roney,[74] H. R. Band,[75] S. Dasu,[75] M. Datta,[75] A. M. Eichenbaum,[75] H. Hu,[75] J. R. Johnson,[75] P. E. Kutter,[75] H. Li,[75] R. Liu,[75] F. Di Lodovico,[75] A. Mihalyi,[75] A. K. Mohapatra,[75] Y. Pan,[75] R. Prepost,[75] S. J. Sekula,[75] J. H. von Wimmersperg-Toeller,[75] J. Wu,[75] S. L. Wu,[75] Z. Yu,[75] and H. Neal[76]

(The *BABAR* Collaboration)

[1]*Laboratoire de Physique des Particules, F-74941 Annecy-le-Vieux, France*
[2]*Università di Bari, Dipartimento di Fisica and INFN, I-70126 Bari, Italy*
[3]*Institute of High Energy Physics, Beijing 100039, China*
[4]*University of Bergen, Inst. of Physics, N-5007 Bergen, Norway*
[5]*Lawrence Berkeley National Laboratory and University of California, Berkeley, CA 94720, USA*
[6]*University of Birmingham, Birmingham, B15 2TT, United Kingdom*
[7]*Ruhr Universität Bochum, Institut für Experimentalphysik 1, D-44780 Bochum, Germany*
[8]*University of Bristol, Bristol BS8 1TL, United Kingdom*
[9]*University of British Columbia, Vancouver, BC, Canada V6T 1Z1*
[10]*Brunel University, Uxbridge, Middlesex UB8 3PH, United Kingdom*
[11]*Budker Institute of Nuclear Physics, Novosibirsk 630090, Russia*
[12]*University of California at Irvine, Irvine, CA 92697, USA*
[13]*University of California at Los Angeles, Los Angeles, CA 90024, USA*
[14]*University of California at San Diego, La Jolla, CA 92093, USA*
[15]*University of California at Santa Barbara, Santa Barbara, CA 93106, USA*
[16]*University of California at Santa Cruz, Institute for Particle Physics, Santa Cruz, CA 95064, USA*
[17]*California Institute of Technology, Pasadena, CA 91125, USA*
[18]*University of Cincinnati, Cincinnati, OH 45221, USA*
[19]*University of Colorado, Boulder, CO 80309, USA*
[20]*Colorado State University, Fort Collins, CO 80523, USA*
[21]*Technische Universität Dresden, Institut für Kern- und Teilchenphysik, D-01062 Dresden, Germany*

^{22}Ecole Polytechnique, LLR, F-91128 Palaiseau, France

^{23}University of Edinburgh, Edinburgh EH9 3JZ, United Kingdom

^{24}Università di Ferrara, Dipartimento di Fisica and INFN, I-44100 Ferrara, Italy

^{25}Florida A&M University, Tallahassee, FL 32307, USA

^{26}Laboratori Nazionali di Frascati dell'INFN, I-00044 Frascati, Italy

^{27}Università di Genova, Dipartimento di Fisica and INFN, I-16146 Genova, Italy

^{28}Harvard University, Cambridge, MA 02138, USA

^{29}Imperial College London, London, SW7 2BW, United Kingdom

^{30}University of Iowa, Iowa City, IA 52242, USA

^{31}Iowa State University, Ames, IA 50011-3160, USA

^{32}Laboratoire de l'Accélérateur Linéaire, F-91898 Orsay, France

^{33}Lawrence Livermore National Laboratory, Livermore, CA 94550, USA

^{34}University of Liverpool, Liverpool L69 3BX, United Kingdom

^{35}Queen Mary, University of London, E1 4NS, United Kingdom

^{36}University of London, Royal Holloway and Bedford New College, Egham, Surrey TW20 0EX, United Kingdom

^{37}University of Louisville, Louisville, KY 40292, USA

^{38}University of Manchester, Manchester M13 9PL, United Kingdom

^{39}University of Maryland, College Park, MD 20742, USA

^{40}University of Massachusetts, Amherst, MA 01003, USA

^{41}Massachusetts Institute of Technology, Laboratory for Nuclear Science, Cambridge, MA 02139, USA

^{42}McGill University, Montréal, QC, Canada H3A 2T8

^{43}Università di Milano, Dipartimento di Fisica and INFN, I-20133 Milano, Italy

^{44}University of Mississippi, University, MS 38677, USA

^{45}Université de Montréal, Laboratoire René J. A. Lévesque, Montréal, QC, Canada H3C 3J7

^{46}Mount Holyoke College, South Hadley, MA 01075, USA

^{47}Università di Napoli Federico II, Dipartimento di Scienze Fisiche and INFN, I-80126, Napoli, Italy

^{48}NIKHEF, National Institute for Nuclear Physics and High Energy Physics, NL-1009 DB Amsterdam, The Netherlands

^{49}University of Notre Dame, Notre Dame, IN 46556, USA

^{50}Oak Ridge National Laboratory, Oak Ridge, TN 37831, USA

^{51}Ohio State University, Columbus, OH 43210, USA

^{52}University of Oregon, Eugene, OR 97403, USA

^{53}Università di Padova, Dipartimento di Fisica and INFN, I-35131 Padova, Italy

^{54}Universités Paris VI et VII, Lab de Physique Nucléaire H. E., F-75252 Paris, France

^{55}Università di Pavia, Dipartimento di Elettronica and INFN, I-27100 Pavia, Italy

^{56}University of Pennsylvania, Philadelphia, PA 19104, USA

^{57}Università di Pisa, Dipartimento di Fisica, Scuola Normale Superiore and INFN, I-56127 Pisa, Italy

^{58}Prairie View A&M University, Prairie View, TX 77446, USA

^{59}Princeton University, Princeton, NJ 08544, USA

^{60}Università di Roma La Sapienza, Dipartimento di Fisica and INFN, I-00185 Roma, Italy

^{61}Universität Rostock, D-18051 Rostock, Germany

^{62}Rutherford Appleton Laboratory, Chilton, Didcot, Oxon, OX11 0QX, United Kingdom

^{63}DSM/Dapnia, CEA/Saclay, F-91191 Gif-sur-Yvette, France

^{64}University of South Carolina, Columbia, SC 29208, USA

^{65}Stanford Linear Accelerator Center, Stanford, CA 94309, USA

^{66}Stanford University, Stanford, CA 94305-4060, USA

^{67}State Univ. of New York, Albany, NY 12222, USA

^{68}University of Tennessee, Knoxville, TN 37996, USA

^{69}University of Texas at Austin, Austin, TX 78712, USA

^{70}University of Texas at Dallas, Richardson, TX 75083, USA

^{71}Università di Torino, Dipartimento di Fisica Sperimentale and INFN, I-10125 Torino, Italy

^{72}Università di Trieste, Dipartimento di Fisica and INFN, I-34127 Trieste, Italy

^{73}Vanderbilt University, Nashville, TN 37235, USA

^{74}University of Victoria, Victoria, BC, Canada V8W 3P6

^{75}University of Wisconsin, Madison, WI 53706, USA

^{76}Yale University, New Haven, CT 06511, USA

(Dated: July 10, 2003)

With a sample of approximately 89 million $B\overline{B}$ pairs collected with the BABAR detector, we perform a search for B meson decays into pairs of charmless vector mesons (ϕ, ρ, and K^*). We measure the branching fractions, determine the degree of longitudinal polarization, and search for CP violation asymmetries in the processes $B^+ \to \phi K^{*+}$, $B^0 \to \phi K^{*0}$, $B^+ \to \rho^0 K^{*+}$, and $B^+ \to \rho^0 \rho^+$. We also set an upper limit on the branching fraction for the decay $B^0 \to \rho^0 \rho^0$.

Charmless B meson decays provide an opportunity to measure the weak-interaction phases arising from the elements of the Cabibbo-Kobayashi-Maskawa (CKM) quark-mixing matrix [1] and to search for phenomena outside the standard model, including charged Higgs bosons and supersymmetric particles [2].

The decays to two vector particles are of special interest because their angular distributions reflect both strong and weak interaction dynamics [3]. The asymmetries constructed from the number of B decays with each flavor and with each sign of a triple product are sensitive to CP violation or to final state interactions (FSI) [4]. The triple product is defined as $(\mathbf{q_1} - \mathbf{q_2}) \cdot \mathbf{p_1} \times \mathbf{p_2}$, where $\mathbf{q_1}$ and $\mathbf{q_2}$ are the momenta of the two vector particles in the B frame and $\mathbf{p_1}$ and $\mathbf{p_2}$ represent their polarization vectors.

The first evidence for the decays of B mesons to pairs of charmless vector mesons was provided by the CLEO [5] and $BABAR$ [6] experiments with the observation of $B \to \phi K^*$ decays. The CLEO experiment also set upper limits on the B decay rates for several other vector-vector final states [7]. The BELLE experiment recently announced observation of $B^+ \to \rho^0 \rho^+$ [8].

In this analysis, we use the data collected with the $BABAR$ detector [9] at the PEP-II asymmetric-energy e^+e^- collider [10]. These data represent an integrated luminosity of 81.9 fb^{-1}, corresponding to 88.9 million $B\overline{B}$ pairs, at the $\Upsilon(4S)$ resonance (on-resonance) and 9.6 fb^{-1} approximately 40 MeV below this energy (off-resonance). The $\Upsilon(4S)$ resonance occurs at the e^+e^- center-of-mass (c.m.) energy, $\sqrt{s}$, of 10.58 GeV.

Charged-particle momenta are measured in a tracking system that is a combination of a silicon vertex tracker (SVT) consisting of five double-sided detectors and a 40-layer central drift chamber (DCH), both operating in a 1.5 T solenoidal magnetic field. Charged-particle identification is provided by the energy loss (dE/dx) in the tracking devices (SVT and DCH) and by an internally reflecting ring-imaging Cherenkov detector (DIRC) covering the central region. Photons are detected by a CsI(Tl) electromagnetic calorimeter.

We search for charmless vector-vector B meson decays involving ϕ, ρ, and $K^*(892)$ resonances. The event selection and analysis technique have been discussed earlier [6]. We fully reconstruct the charged and neutral decay products including the intermediate states $\phi \to K^+K^-$, $K^{*0} \to K^+\pi^-$ and $K^0\pi^0$, $K^{*+} \to K^+\pi^0$ and $K^0\pi^+$, $\rho^0 \to \pi^+\pi^-$, $\rho^+ \to \pi^+\pi^0$, with $\pi^0 \to \gamma\gamma$ and $K^0 \to K_S^0 \to \pi^+\pi^-$, where inclusion of the charge conjugate states is implied. Candidate charged tracks are required to originate from the interaction point. Looser criteria are applied to tracks forming K_S^0 candidates, which are required to satisfy $|m_{\pi^+\pi^-} - m_{K^0}| < 12$ MeV with the cosine of the angle between their reconstructed flight and momentum directions greater than 0.995, and the measured proper decay time greater than 5 times its un-

certainty. Charged-particle identification provides separation of kaon tracks from pion and proton tracks.

We reconstruct π^0 mesons from pairs of photons, each with a minimum energy of 30 MeV. The invariant mass of the π^0 candidates is required to be within 15 MeV of the nominal mass. The helicity angle of a ϕ, K^*, or ρ is defined as the angle between the momentum ($\mathbf{p_1}$ or $\mathbf{p_2}$) of one of its two daughters (K^+, K, or π^+, respectively) in the resonance rest frame and the momentum ($\mathbf{q_1}$ or $\mathbf{q_2}$) of the resonance in the B frame. To suppress combinatorial background with low-energy π^0 candidates we restrict the $K^* \to K\pi^0$ and $\rho^+ \to \pi^+\pi^0$ helicity angle θ range to $\cos\theta < +0.5$.

We identify B meson candidates kinematically using two nearly independent variables [9]: the beam-energy-substituted mass $m_{\mathrm{ES}} = [(s/2 + \mathbf{p_i} \cdot \mathbf{p}_B)^2/E_i^2 - \mathbf{p}_B^2]^{1/2}$ and the energy difference $\Delta E = (E_i E_B - \mathbf{p_i} \cdot \mathbf{p}_B - s/2)/\sqrt{s}$, where $(E_i, \mathbf{p_i})$ is the initial state four-momentum obtained from the beam momenta, and $(E_B, \mathbf{p}_B)$ is the four-momentum of the reconstructed B candidate. Our initial selection requires $m_{\mathrm{ES}} > 5.2$ GeV and $|\Delta E| < 0.2$ GeV.

To reject the dominant quark-antiquark continuum background, we require $|\cos\theta_T| < 0.8$, where θ_T is the angle between the B-candidate thrust axis and that of the rest of the tracks and neutral clusters in the event, calculated in the c.m. frame. We also construct a Fisher discriminant that combines eleven event-shape variables defined in the c.m. frame [6, 11].

Monte Carlo (MC) simulation [12] demonstrates that contamination from other B decays is negligible for the modes with a narrow ϕ resonance and is relatively small for other charmless B decay modes. We achieve further suppression of B-decay background by removing signal candidates that have decay products consistent with $D \to K\pi, K\pi\pi$ decays. The remaining small background coming from B decays (about 6% of the total background) is taken into account in the fit described below. In this analysis we do not explicitly provide a fit component for other partial waves with the same final-state particles selected within vector resonance mass windows.

We use an unbinned, extended maximum-likelihood (ML) fit [6] to extract signal yields, asymmetries, and angular polarizations simultaneously. We define the likelihood $\mathcal{L}_i$ for each event candidate i as the sum of $n_{jk}\mathcal{P}_j(\vec{x}_i; \vec{\alpha})$ over three event categories j, where $\mathcal{P}_j(\vec{x}_i; \vec{\alpha})$ are the probability density functions (p.d.f.) for measured variables $\vec{x}_i$, n_{jk} are the yields to be extracted from the fit, and k is the measured tag (1 or 2, as defined for asymmetry measurements later). There are three categories: signal ($j = 1$), continuum $q\overline{q}$ ($j = 2$), and $B\overline{B}$ combinatorial background ($j = 3$). The fixed numbers $\vec{\alpha}$ parameterize the expected distributions of measured variables in each category. They are extracted from MC simulation, on-resonance ΔE-m_{ES} sidebands, and off-resonance data.

TABLE I: Summary of results for the measured B-decay modes; ε denotes the reconstruction efficiency and $\varepsilon_{\rm tot}$ the total efficiency including daughter branching fractions, $n_{\rm sig}$ is the fitted number of signal events, $\mathcal{B}$ is the branching fraction, f_L is the longitudinal polarization, and $\mathcal{A}_{CP}$ is the signal charge asymmetry. The decay channels of K^* are shown when more than one final state is measured for the same B decay mode. All results include systematic errors, which are quoted following the statistical errors. The errors are combined for the reconstruction efficiency. The upper limit on the $B^0 \to \rho^0\rho^0$ branching fraction is given at 90% confidence level including systematic uncertainties and conservatively assuming the efficiency for $f_L = 1$.

Mode	ε (%)	$\varepsilon_{\rm tot}$ (%)	$n_{\rm sig}$	$\mathcal{B}$ ($\times 10^{-6}$)	f_L	$\mathcal{A}_{CP}$
ϕK^{*+}	–	5.0	–	$12.7\,^{+2.2}_{-2.0}\pm1.1$	$0.46\pm0.12\pm0.03$	$+0.16\pm0.17\pm0.03$
$\to K^0\pi^+$	23.9 ± 2.1	2.7	$33.3^{+7.2}_{-6.4}\pm1.2$	$13.9\,^{+3.0}_{-2.7}\pm1.2$	$0.50\,^{+0.14}_{-0.15}\pm0.03$	$-0.02\pm0.20\pm0.03$
$\to K^+\pi^0$	14.3 ± 1.4	2.3	$22.3^{+7.5}_{-6.5}\pm3.2$	$10.7\,^{+3.6}_{-3.1}\pm1.8$	$0.40\,^{+0.20}_{-0.19}\pm0.06$	$+0.63\,^{+0.25}_{-0.31}\pm0.05$
ϕK^{*0}	–	10.3	–	$11.2\pm1.3\pm0.8$	$0.65\pm0.07\pm0.02$	$+0.04\pm0.12\pm0.02$
$\to K^+\pi^-$	29.7 ± 2.6	9.7	$101\,^{+12}_{-11}\pm3$	$11.7\pm1.4\pm0.8$	$0.64\pm0.07\pm0.02$	$+0.04\pm0.12\pm0.02$
$\to K^0\pi^0$	10.5 ± 1.0	0.6	$2.0^{+3.4}_{-1.3}\pm0.6$	$3.8\,^{+6.6}_{-2.5}\pm1.1$	$1.00\,^{+0.00}_{-0.66}\pm0.25$	–
$\rho^0 K^{*+}$	–	4.8	–	$10.6^{+3.0}_{-2.6}\pm2.4$	$0.96\,^{+0.04}_{-0.15}\pm0.04$	$+0.20\,^{+0.32}_{-0.29}\pm0.04$
$\to K^0\pi^+$	12.3 ± 2.0	2.8	$35.7^{+11.8}_{-11.0}\pm3.6$	$14.3^{+4.7}_{-4.4}\pm2.9$	$0.90\,^{+0.10}_{-0.16}\pm0.04$	$+0.17\,^{+0.34}_{-0.31}\pm0.04$
$\to K^+\pi^0$	6.0 ± 1.4	2.0	$8.5^{+8.2}_{-6.6}\pm5.2$	$4.8^{+4.6}_{-3.7}\pm3.2$	$1.00\,^{+0.00}_{-0.20}\pm0.03$	$+0.28\,^{+0.72}_{-0.82}\pm0.19$
$\rho^0\rho^+$	4.7 ± 0.9	4.6	$93\,^{+24}_{-22}\pm10$	$22.5^{+5.7}_{-5.4}\pm5.8$	$0.97\,^{+0.03}_{-0.07}\pm0.04$	$-0.19\pm0.23\pm0.03$
$\rho^0\rho^0$	17.6 ± 1.5	17.6	$9.7^{+11.9}_{-9.4}\pm2.0$	< 2.1	–	–

The fit input variables $\vec{x}_i$ are ΔE, $m_{\rm ES}$, Fisher discriminant, invariant masses of the candidate K^* and ϕ (or ρ) resonances, and the K^* and ϕ (or ρ) helicity angles θ_1 and θ_2. The correlations among the fit input variables in the data and signal MC are found to be small (typically less than 5%), except for angular correlations in the signal as discussed below. The p.d.f. $\mathcal{P}_j(\vec{x}_i;\vec{\alpha})$ for a given candidate i is the product of the p.d.f.'s for each of the variables and a joint p.d.f. for the helicity angles, which accounts for the angular correlations in the signal and for detector acceptance effects. We integrate over the angle between the decay planes of the two vector-particle decays, leaving a p.d.f. that depends only on the two helicity angles and the unknown longitudinal polarization fraction $f_L \equiv \Gamma_L/\Gamma$. The differential decay width [3] $d^2\Gamma/d\cos\theta_1 d\cos\theta_2$ is

$$\frac{9\Gamma}{4}\left\{\frac{1}{4}(1-f_L)\sin^2\theta_1\sin^2\theta_2 + f_L\cos^2\theta_1\cos^2\theta_2\right\}. \quad (1)$$

To describe the signal distributions, we use Gaussian functions for the parameterization of the p.d.f.'s for ΔE and $m_{\rm ES}$, and a relativistic P-wave Breit-Wigner distribution, convoluted with a Gaussian resolution function, for the resonance masses. For the background, we use low-degree polynomials or, in the case of $m_{\rm ES}$, an empirical phase-space function [13]. The background parameterizations for resonance masses also include a resonant component to account for resonance production in the

continuum. The background helicity-angle distribution is again separated into contributions from combinatorial background and from real vector mesons, both described by polynomials. The p.d.f. for the Fisher discriminant is represented by a Gaussian distribution with different widths above and below the mean.

We denote $Q_{\rm tp}$ as the sign of the triple product and $Q_{\rm ch}$ as the B-flavor sign ($Q_{\rm ch} = +1$ for $\overline{B}$ and $Q_{\rm ch} = -1$ for B). The charged B is intrinsically flavor-tagged. The flavor of a neutral B is determined from the charge of the kaon in the final states with the $K^{*0} \to K^+\pi^-$, but is undetermined for the decay mode $K^{*0} \to K^0\pi^0$ and for the decay $B^0 \to \rho^0\rho^0$.

We rewrite the event yields n_{jk} (k=1,2) in each category j in terms of the asymmetry $\mathcal{A}_j$ and the total event yield n_j: $n_{j1} = n_j\times(1+\mathcal{A}_j)/2$ and $n_{j2} = n_j\times(1-\mathcal{A}_j)/2$. We define three signal asymmetries using the tags k: $\mathcal{A}_{CP}$ ($k = 1$ for $Q_{\rm ch} > 0$, $k = 2$ for $Q_{\rm ch} < 0$), $\mathcal{A}_{\rm tp}$ ($k = 1$ for $Q_{\rm ch} \times Q_{\rm tp} > 0$, $k = 2$ for $Q_{\rm ch} \times Q_{\rm tp} < 0$), and $\mathcal{A}_{\rm sp}$ ($k = 1$ for $Q_{\rm tp} > 0$, $k = 2$ for $Q_{\rm tp} < 0$). A non-zero value for $\mathcal{A}_{CP}$ would provide evidence for direct-CP violation, non-zero $\mathcal{A}_{\rm tp}$ indicates CP violation even in the absence of FSI, and $\mathcal{A}_{\rm sp}$ is sensitive to strong-interaction phases [4].

We allow for multiple candidates in a given event by assigning to each a weight of $1/N_i$, where N_i is the number of candidates in the same event. The extended likelihood

for a sample of N_{cand} candidates is

$$\mathcal{L} = \exp\left(-\sum_{j=1}^{3} n_j\right) \prod_{i=1}^{N_{\text{cand}}} \exp\left(\frac{\ln \mathcal{L}_i}{N_i}\right). \qquad (2)$$

The event yields n_j, asymmetries $\mathcal{A}_j$, and polarization f_L are obtained by minimizing the quantity $\chi^2 \equiv -2\ln\mathcal{L}$. The dependence of χ^2 on a fit parameter n_j, $\mathcal{A}_j$, or f_L is obtained with the other fit parameters floating, their values are constrained to the physical range $0 \leq f_L \leq 1$ and $0 \leq n_j$. We quote statistical errors corresponding to unit change in χ^2. When more than one K^* decay channel is measured for the same B decay, the channels are combined by adding their χ^2 distributions for n_j, $\mathcal{A}_j$, or f_L. The statistical significance of a signal is defined as the square root of the change in χ^2 when constraining the number of signal events to zero in the likelihood fit. If no significant event yield is observed, we quote an upper limit for the branching fraction obtained by integrating the normalized likelihood distribution. Performance of the ML fit is tested with generated MC and control samples.

The results of our maximum likelihood fits are summarized in Table I. For the branching fractions, we assume equal production rates of $B^0\overline{B}^0$ and B^+B^-. We find significant signals in $\rho^0 K^{*+}$ (4.8σ), $\rho^0\rho^+$ (6.1σ), and in both ϕK^* (above 10σ each) decay modes. We measure the charge asymmetries and longitudinal polarizations in the above modes. The projections of the fit results are shown in Fig. 1 and 2. The asymmetries involving triple products are obtained from separate fits. The results are shown in Table II.

Systematic uncertainties in the ML fit originate from assumptions about the p.d.f.'s. We vary the p.d.f. parameters within their respective uncertainties, and derive the associated systematic errors. The signals remain statistically significant under these variations. Additional systematic errors in the number of signal events originate from uncertainty in the background component for ρK^* that peaks in m_{ES}, where we take the uncertainties to be the estimated values.

The systematic errors in the efficiencies are for track

TABLE II: Summary of asymmetry results with triple products discussed in the text.

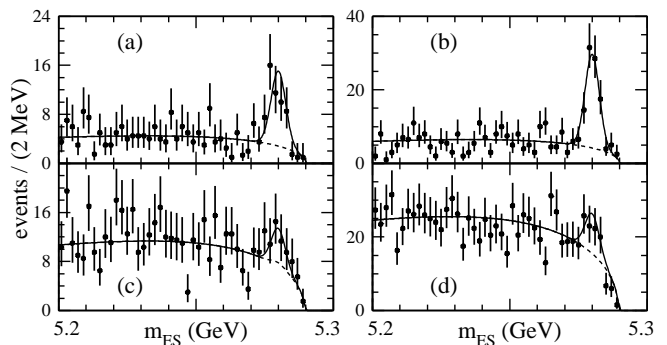| Mode	$\mathcal{A}_{\text{tp}}$	$\mathcal{A}_{\text{sp}}$
ϕK^{*+}	$-0.02 \pm 0.18 \pm 0.03$	$-0.04 \pm 0.18 \pm 0.03$
ϕK^{*0}	$+0.06 \pm 0.12 \pm 0.02$	$+0.07 \pm 0.12 \pm 0.02$
$\rho^0 K^{*+}$	$+0.03 \pm 0.29 \pm 0.03$	$+0.28 \,^{+0.38}_{-0.33} \pm 0.04$
$\rho^0\rho^+$	$+0.09 \pm 0.24 \pm 0.04$	$-0.23 \pm 0.24 \pm 0.04$

FIG. 1: Projections of the multidimensional fit onto the variable m_{ES} for (a) $B^+ \to \phi K^{*+}$, (b) $B^0 \to \phi K^{*0}$, (c) $B^+ \to \rho^0 K^{*+}$, and (d) $B^+ \to \rho^0\rho^+$ candidates after a requirement on the signal-to-background probability ratio $\mathcal{P}_{\text{sig}}/\mathcal{P}_{\text{bkg}}$ with the p.d.f. for m_{ES} excluded. The points with error bars show the data, the solid (dashed) line shows the signal-plus-background (background only) p.d.f. projection.
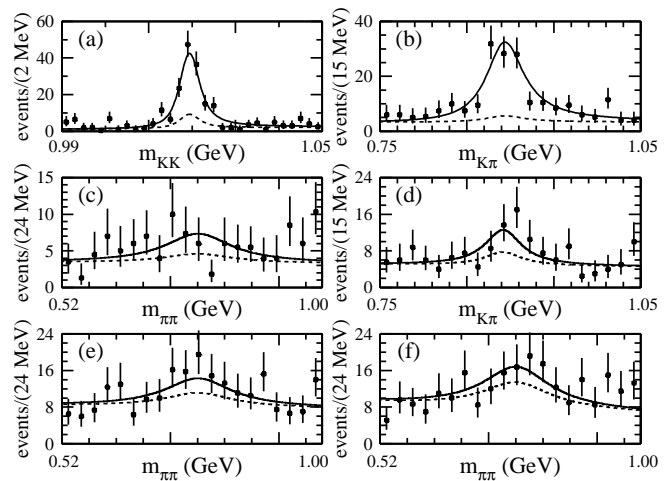

FIG. 2: Invariant mass projections (a) ϕ, (b) K^* for $B \to \phi K^*$; (c) ρ^0, (d) K^{*+} for $B^+ \to \rho^0 K^{*+}$; (e) ρ^0, (f) ρ^+ for $B^+ \to \rho^0\rho^+$ candidates after a requirement on the signal-to-background probability ratio $\mathcal{P}_{\text{sig}}/\mathcal{P}_{\text{bkg}}$ with the p.d.f. for mass excluded. For point and line definitions see Fig. 1.

finding (0.8% per track), particle identification (2% per track), and K^0_S and π^0 reconstruction (5% each). Other minor systematic effects are from event-selection criteria, daughter branching fractions [14], MC statistics, and number of B mesons. We account for the fake combinations in signal events passing the selection criteria with a systematic uncertainty of 3–12%, depending on the mode. The reconstruction efficiency depends on the decay polarization. We calculate the efficiencies using the polarization measured in each decay mode [15] (combined for the two ϕK^* modes) and assign a systematic error corresponding to the total polarization measurement error. The $B^0 \to \rho^0\rho^0$ branching fraction limit incorporates uncertainties in the p.d.f.'s and in the re-

construction efficiency, while we conservatively assume $f_L = 1$ for the efficiency (which is 29% for $f_L = 0$ and 18% for $f_L = 1$).

In the polarization and asymmetry measurements, we again include systematic errors from p.d.f. variations that account for uncertainties in the detector acceptance and background parameterizations. The biases from the finite resolution in helicity angle measurement and dilution due to the presence of the fake combinations are studied with MC simulation and are accounted for with a systematic error of 0.02 for polarization. We find the uncertainty on the charge asymmetry due to the track reconstruction efficiency to be less than 0.02 [6]. The asymmetry measurements are corrected by the small dilution factors.

In summary, we have observed the decays $B^+ \rightarrow \phi K^{*+}$, $B^0 \rightarrow \phi K^{*0}$, $B^+ \rightarrow \rho^0 K^{*+}$, and $B^+ \rightarrow \rho^0 \rho^+$, measured their branching fractions and longitudinal polarizations, and looked for asymmetries sensitive to CP violation and FSI. These results supersede the earlier $BABAR$ measurements of the $B \rightarrow \phi K^*$ [6]. Our asymmetry results rule out a significant part of the physical region, providing constraints on models with hypothetical particles, but are not yet sufficiently precise to allow detailed comparison with standard model predictions. Our measurement of longitudinal polarization is of interest for the study of decay dynamics.

[*] Also with Università di Perugia, Perugia, Italy
[†] Also with Università della Basilicata, Potenza, Italy
[‡] Also with IFIC, Instituto de Física Corpuscular, CSIC-Universidad de Valencia, Valencia, Spain
[§] Deceased

[1] M. Kobayashi, T. Maskawa, Prog. Theor. Phys. **49**, 652 (1973).
[2] Y. Grossman, M.P. Worah, Phys. Lett. B **395**, 241 (1997); D. London, A. Soni, Phys. Lett. B **407**, 61 (1997).
[3] G. Kramer, W.F. Palmer, Phys. Rev. D **45**, 193 (1992); H.-Y. Cheng, K.-C. Yang, Phys. Lett. B **511**, 40 (2001); C.-H. Chen, Y.-Y. Keum, H.-n. Li, Phys. Rev. D **66**, 054013 (2002).
[4] G. Valencia, Phys. Rev. D **39**, 3339 (1989); W. Bensalem, D. London, Phys. Rev. D **64**, 116003 (2001).
[5] CLEO Collaboration, R.A. Briere et al., Phys. Rev. Lett. **86**, 3718 (2001).
[6] BABAR Collaboration, B. Aubert et al., Phys. Rev. Lett. **87**, 151801 (2001); BABAR Collaboration, B. Aubert et al., Phys. Rev. D **65**, 051101 (2002).
[7] CLEO Collaboration, R. Godang et al., Phys. Rev. Lett. **88**, 021802 (2002).
[8] BELLE Collaboration, J. Zhang et al., BELLE-2003-6, hep-ex/0306007, submitted to Phys. Rev. Lett.
[9] BABAR Collaboration, B. Aubert et al., Nucl. Instrum. Methods **A479**, 1 (2002).
[10] PEP-II Conceptual Design Report, SLAC-R-418 (1993).
[11] CLEO Collaboration, D.M. Asner et al., Phys. Rev. D **53**, 1039 (1996).
[12] The BABAR detector Monte Carlo simulation is based on GEANT: R. Brun et al., CERN DD/EE/84-1.
[13] ARGUS Collaboration, H. Albrecht et al., Phys. Lett. B **241**, 278 (1990).
[14] Particle Data Group, K. Hagiwara et al., Phys. Rev. D **66**, 010001 (2002).
[15] Preliminary BABAR results prior to polarization measurements assumed $f_L = 0.5$, leading to a smaller branching fraction. The systematic error on the branching ratio due to the unknown polarization was underestimated in the preliminary result.